

Correction of Continuous Wave Signals for Pulsar Glitch Induced Phase Shifts

J. Elliot Adelman

Hamilton College, Clinton NY, 13323

Christiano Palomba

INFN, Roma

1. Abstract

The search for direct observation of gravitational waves remains an important avenue of research in experimental physics. Among possible sources for measurable gravitational radiation are pulsars. One problem with these sources, however, is the tendency to exhibit glitches, which are predicted to cause unpredictable phase discontinuities in the gravitational wave signal, compromising attempts at coherent analysis. This research reports on the development and testing of a MATLAB program designed to correct for such phase discontinuities.

2. Introduction

2.1 Gravitational Waves

A major deficiency of the classical theory of gravitation, recognized by Newton himself, is its reliance on action at a distance to explain the transmission of information. General Relativity ameliorates this issue by proposing the existence of gravitational radiation as a means of mediating information about distant masses. These waves, in actuality propagating oscillations in the underlying curvature, emerge from examination of a metric constructed from Minkowski space and a small non-flat perturbative tensor to first order in the perturbing piece¹.

The small relative size of the gravitational constant, G , limits current hopes of direct gravitational wave (GW) detection to massive, relativistic objects located in outer space. As of yet, no experiment has directly observed gravitational radiation. However, observations of the decrease in orbital period of binary pulsars, starting with PSR 1913 + 16 in 1978, are consistent with the emission of GWs as predicted by general relativity². The quest towards the direct observation of this radiation remains an important facet of experimental gravitational physics.

2.2 The Detectors: LIGO, VIRGO, and GEO600

Current efforts for gravitational wave observation are focused on ground-based interferometers, three of which are in existence: LIGO in the United States, GEO600 in Germany, and VIRGO in Italy. At the moment, the LIGO and VIRGO apparati are in the process of undergoing major upgrades into Advanced LIGO and Advanced VIRGO; these improvements are hoped to facilitate the direct observation of gravitational wave signals.³ The author's research this summer dealt entirely with data produced by the VIRGO detector. The specifics of these apparati and the engineering involved in their construction are beyond the scope of this report,

but are documented thoroughly in the outstanding literature. Basically, the detectors are Michelson interferometers with two Fabry-Perot cavities ranging in length from 600 m (GEO600) to 4 km (LIGO) for which great pains have been taken to isolate the cavities from environmental contamination⁴⁵⁶.

2.3 Continuous Wave Sources

Due to conservation of mass and momentum, the leading order contribution to gravitational radiation under general relativity comes from the third derivative of a mass-energy distribution's quadrupole moment⁷. This combined with the aforementioned small magnitudes of the expected signals gives several groups of possible candidates for producing detectable GWs, including burst signals produced for instance by a stellar merger. The author's research focused on continuous wave (CW) sources for gravitational radiation; this category, encompassing sources such as compact binaries and asymmetric pulsars⁸, is further divided into blind and targeted searches, which consist of full-sky and specific source examinations, respectively. This research focused on targeted CW signals, specifically those emitted by rapidly rotating asymmetric neutron stars. In this case, the theoretical signals at the detector (after corrections for Doppler and other effects) are completely determined by only four source parameters (four degrees of freedom)⁹; the nature of these parameters is discussed in section 3.3 below.

3. Theory

3.1 The Five-Vector Formalism

After data cleaning, the CW signal from the targeted pulsar is monochromatic with frequency ω , but appears as spread over five frequencies (ω , $\omega \pm \Omega$, $\omega \pm 2\Omega$, where Ω is the earth sidereal frequency) due to earth's rotation. Thus, all information relating to four source parameters may be gleaned from just the Fourier transforms of the cleaned data at the five frequencies. The result of these transformations is stored in the form of a *data five-vector* (X), and has ten degrees of freedom (since the values at each of the five frequencies are complex). In the general case, X may be written as:

$$X = A + N \quad (1)$$

where A is the signal five vector and N the noise. Separating these components of X is accomplished with a match filter, in which the templates corresponding to the plus and cross wave polarizations are produced taking into account the same gaps as are present in the raw data. The resulting estimated plus and cross amplitudes, h_+ and h_x , are then used in calculating the four source parameters.¹⁰

3.2 Coherence and the 5N Vectors

In order to measure the reliability of the detection, analysis proceeds with the calculation a *coherence* (c) following the determination of the scaled signal plus and cross templates. The values c is defined by:

$$c = \left| \tilde{X} \cdot \tilde{A} \right|^2 \quad (2)$$

where the tildes indicate that the signal and data vectors have been normalized; thus c ranges from 0 to 1. Previous simulations indicate that for pure Gaussian noise, the probabilities for values of c follow a β -distribution.¹¹

The utility of the coherence is improved by coherently analyzing multiple data subsets simultaneously, concatenating each of the individual data and signal five-vectors into one large $5N$ vector. This operation does not affect the analysis paradigm discussed (briefly) in 3.1, but vastly reduces susceptibility to false positives, as shown in the figure below (**Figure #1**):

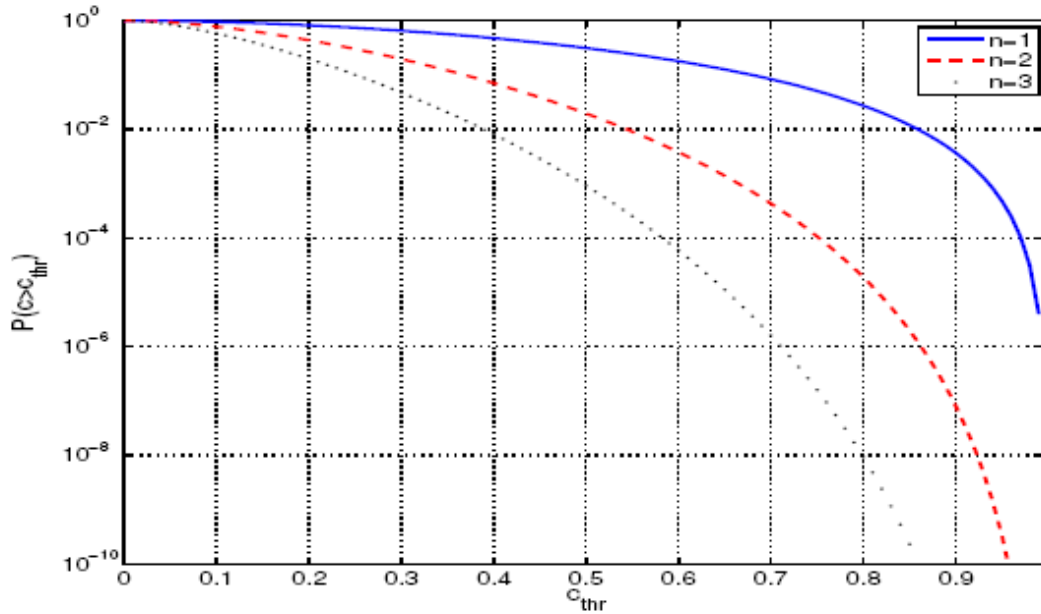


Figure #1: Probability of obtaining a coherence greater than a specified coherence threshold at three different numbers of separate five-vectors included in the analysis for data vectors consisting solely of Gaussian noise.¹²

This coherent $5N$ vector analysis, however, relies on the assumption that the four source parameters (see 3.3, below) are identical for all data sets included in the coherent analysis. Thus, data sets known to have different source parameters must be analyzed independently or "corrected" to have matching parameters.

3.3 Continuous Wave Source Parameters

The GW signals from the pulsar targets for the CW analysis are completely determined by four independent parameters: η , ψ , magnitude, and phase (γ). Once h_+ and h_x are calculated, the overall magnitude is simply the square root of the sum of the component squares. The value for η describes the ratio of the semi-major axis to the semi-minor axis polarization ellipse, while ψ indicates the polarization ellipse's orientation; both these values may be estimated from the two algebraic combinations of the polarization coefficients that are independent of γ . Finally, the overall phase is calculated from the complex ratio between the calculated (data) polarization coefficients and the signal templates produced by the now-specified values for η and ψ .¹³

3.4 Pulsar Glitches

One issue facing pulsars as candidates for targeted CW searches concerns their tendency to exhibit glitches. These glitches are characterized by sudden increases in rotational frequency, followed by a period of gradual relaxation back towards the original frequency. The exact cause of these jumps remains a subject of debate; the current favored theory holds these glitches stem from sudden transfers of angular momentum from the pulsar crust to its superfluid core. Observation of these glitches indicates that they are most common in "young" pulsars (10 kiloyears), and disappear completely after about 20 megayears.¹⁴

Targeted CW searches for gravitational waves are concerned with pulsar glitches because such glitches are present in a number of potential CW sources. For instance, PSR J0537–6910, a possible target located in the Large Magellanic Cloud, has exhibited no fewer than twenty-three glitches during a seven year observation period.¹⁵ Furthermore, due to discontinuous nature of the pulsar glitches, it is assumed that at least the phase, γ , will change as a result, with possible shifts also observed in the other three target source parameters. Due to these shifts, coherent 5N-vector analysis will no longer be possible involving data sets from opposite sides of a recorded glitch.

4. Methods

4.1 Snag and the gd Structure

Current analysis of VIRGO data at INFN Roma is performed using Snag, a MATLAB program designed primarily by Sergio Frasca. In the Snag paradigm, data are stored in the form of a *gd structure*, which consists of the time and data vectors and attached cell arrays containing information pertaining to data collection run. In designing a usable program to correct for phase shifts as a result of observed pulsar glitches, it is essential to ensure that the results fit seamlessly into the existing Snag architecture. Thus, the initial conception of the glitch fixing program envisioned both the input and output as gd structures, with the program performing only a time-series translation to correct for the phase shift (since a phase shift inverse Fourier transforms into a shift of the dependant variable). The final version of the program (see section 5.2) maintained the gd input, but switched to a frequency space (5N vector) output, meaning that in-stream integration of the glitch correction software to the existing Snag architecture will replace the five vector conversion program in the cases of glitchy pulsars.

4.2 Coherence Maximization vs. Inner Product Maximization

The original idea for pulsar glitch correction, as proposed by Astone, et. al.,¹⁶ suggested using a coherence maximization to estimate the parameter shifts between data sets taken before and after a known target pulsar glitch. Starting from (2), this means for $n = 2$ (as in the programs, see section 5 below), we are maximizing:

$$c = \left(\frac{1}{\|X\| \|A\|} \right)^2 |X_1 \cdot A_1 + X_2 \cdot A_2|^2 \quad (3)$$

where the subscripts correspond to the first and second blocks, respectively. Since the overall normalization is meaningless in the optimization, this is equivalent to maximizing:

$$|X_1 \cdot A_1 + X_2 \cdot A_2|^2 \quad (4)$$

or:

$$(X_1 \cdot A_1 + X_2 \cdot A_2)(\overline{X_1 \cdot A_1 + X_2 \cdot A_2}) \quad (5)$$

$$(X_1 \cdot A_1)(\overline{X_1 \cdot A_1}) + (X_2 \cdot A_2)(\overline{X_1 \cdot A_1}) + (X_1 \cdot A_1)(\overline{X_2 \cdot A_2}) + (X_2 \cdot A_2)(\overline{X_2 \cdot A_2}) \quad (6)$$

For the case in which we are correcting only for γ , however, we may make further simplifications, since the correction corresponds to changing X_2 to X_2' , where:

$$X_2' = X_2 e^{i\phi} \quad (7)$$

for an unknown phase, ϕ , that corresponds to the maximization independent variable. Since none of the other five vectors are manipulated during the optimization, we notice that both the first and last terms in (6) are constants independent of ϕ , as the first term does not depend on X_2 while the last term contains after substitution both an $e^{i\phi}$ and an $e^{-i\phi}$ scalar term, whose product is unity. Thus for the case in which we assume the pulsar glitch produces only a change in phase, we optimize:

$$e^{i\phi}(X_2 \cdot A_2)(\overline{X_1 \cdot A_1}) + e^{-i\phi}(X_1 \cdot A_1)(\overline{X_2 \cdot A_2}) \quad (8)$$

Notice that the terms in (8) are complex conjugates; thus, the optimization amounts to maximizing the real part of:

$$e^{i\phi}(X_2 \cdot A_2)(\overline{X_1 \cdot A_1}) \quad (9)$$

The real part of (9) is largest when the complex number $e^{i\phi}(X_2 \cdot A_2)$ has the same phase as $(\overline{X_1 \cdot A_1})$; for the case in which the templates are the same (as is ideally true, since calculating the templates has no overall phase dependence), maximizing the coherence by adjusting ϕ is equivalent to maximizing the inner product between the two data five-vectors (n.b. - the inner product of two complex vectors A and B is defined as the sum of the products of the i th component of A with the complex conjugate of the i th component of B). Thus, instead of maximizing coherence calculations, the programs discussed in Section 5 below maximizes the inner product between the two five vectors in order to determine the phase shift between them.

5. Programs Created

5.1 Program "five_vector_phase.m"

This program, created in MATLAB, ascertains the phase difference between two data five vectors by the inner product maximization method. The backbone of the program is a loop over a user-specified number of phases equally spaced on the interval $(0, 2\pi]$; the program scales the second input vector by each phase evaluates the inner, returning the phase that yields the largest value. Later versions of the program also return the phase shift maxima locations for each of the individual five-vector components, as their magnitudes and spread give information as to the precision of the phase shift recorded. The following flowchart (**Figure #2**) outlines the action of this program:

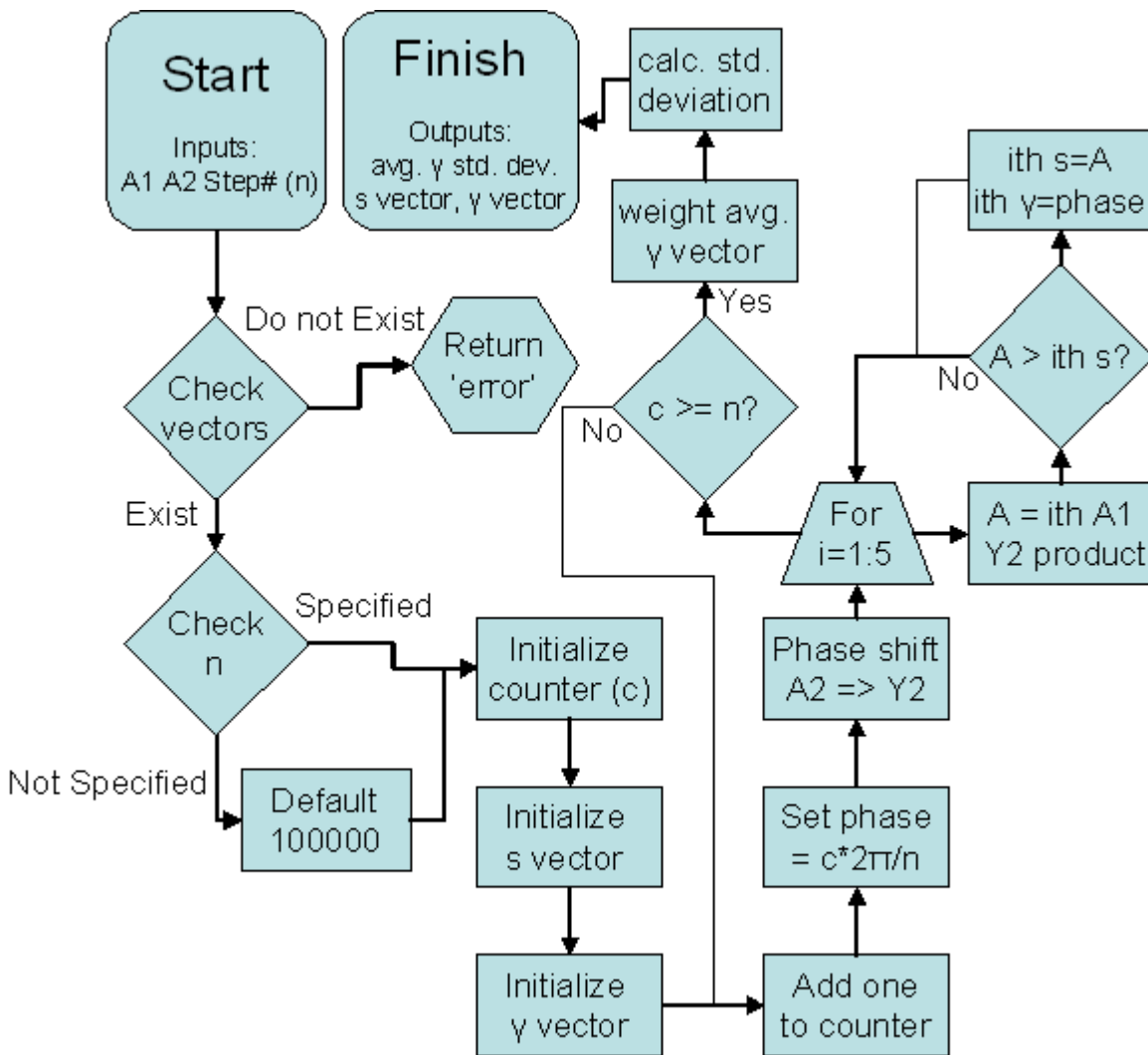


Figure #2: Flowchart outline of the program five_vector_phase.m

5.2 Program "multishift_test.m"

This program (also in MATLAB) represents an extension of five_vector_phase.m, allowing for the possibility of multiple glitches within an otherwise coherent target source data acquisition run. Originally conceived as operating on a single gd, with glitch periods specified by additional vector inputs, the method of operation was amended instead to act on individual gds corresponding to the datasets between the recorded glitch periods. This change allowed for greater generality, in case the pulsar glitch corresponds to a significant change in spin-down or frequency, and also for the use of non-sequential datasets for the purpose of coherence improvement.

The first versions of this program also attempted to correct the phase shift in time space, as noted in section 4.1 above; however, tests of program performance later revealed that this method of storage compromised information about the coherence and signal magnitude, since the five vector templates (A) were now being calculated using an incorrect time. Thus, consistent with the use of five vectors in parameter calculation (as discussed in section 3.3), the final

version of this program stored the correction in the form of five vectors. The following flowchart (**Figure #3**) illustrates the functionality of this final version of `multishift_test.m`:

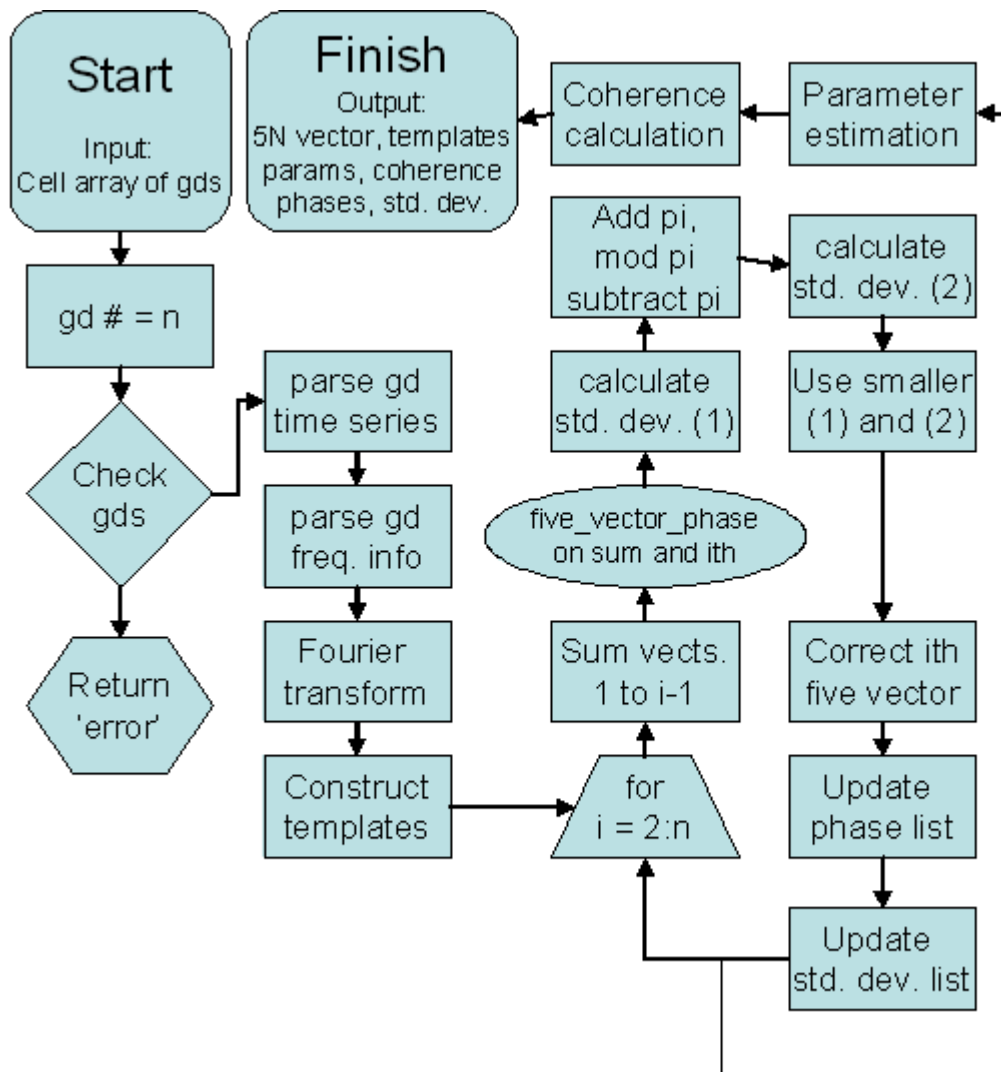


Figure #3: Flowchart outline of program `multishift_test.m`

6. Discussion

6.1 Performance Testing: `five_vector_phase.m`

In order to evaluate the effectiveness of the `five_vector_phase.m` program, a series of three tests were performed using simulated signals. The first, using five vectors with shifts generated manually in frequency space, demonstrated that the program was healthy and able to successfully pinpoint shift magnitude to arbitrary precision. The second tests were performed on five vectors generated from five superimposed finite-length time-space sinusoids with added pseudorandom scaled white Gaussian noise. This test allowed for a probe of expected program performance over a range of signal-to-noise ratios (SNRs), the results of which (**Figure #4**) matched expectations:

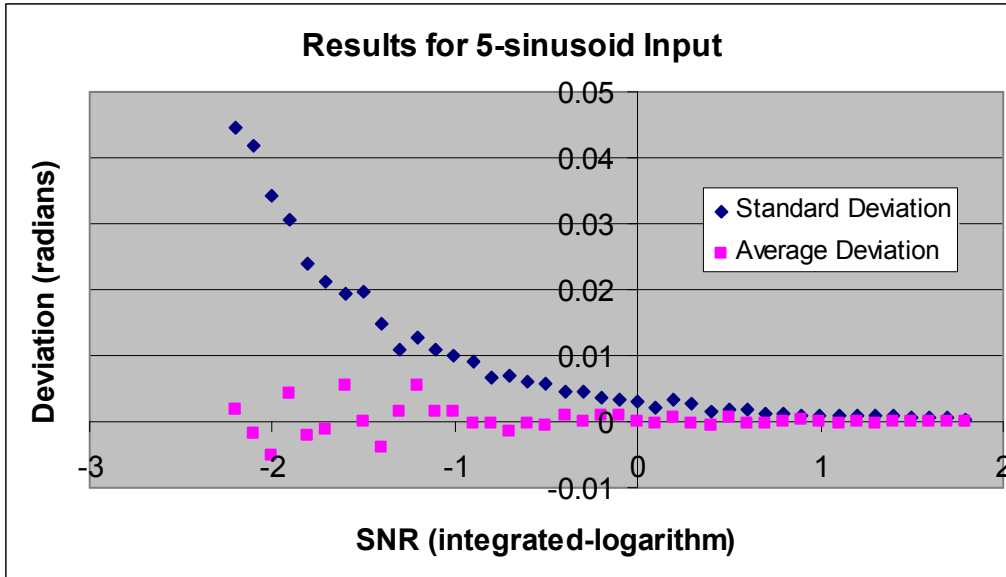


Figure #4: Results for the second test of `five_vector_phase.m`. In this test, forty different randomly generated Gaussian noise sets were added to each of two five-sinusoid inputs that were phase offset by 1 radian. The magnitude of the noise was scaled to give a range of SNRs, and then the phase shifts were tallied. The blue curve shows the standard deviations of these forty shifts (in radians) as a function of SNR, while the magenta curve gives the average of the forty shifts subtracted from 1.

The standard deviation curve, which gives an estimate of the expected discrepancy in shift for any single two five vectors with a given SNR, shows not just the expected logistic shape ("logistic" due to the fact that the shifts are meaningful only modulus 2π , meaning the deviation will asymptote at a value less than π as the SNR approaches zero) but also demonstrates adequate precision (<0.01 radian) over the signal to noise range (-1 to 1, on a logarithmic scale) expected for the eventual corrected VIRGO data, and approaches asymptotically the expected zero at high SNRs. The average deviation also matches predictions; these points should fall within the umbrella of the standard error (which is an estimate of this quantity), with an even distribution about zero (thus displaying no inherent program bias towards either consistently overestimating or underestimating the shift).

The final test simulated VIRGO signals from templates containing the same data holes present in actual raw data, with noise from a recent VIRGO data run serving as the scaled background. This test exposed an immediate flaw; at high SNRs, instead of approaching zero, the calculated shift discrepancy approached a nonzero, positive value several orders of magnitude larger than the expected precision limit due to the finite number of phases tested in the backbone for loop. Eventually, a test comparing the phase shift error calculated from two five vectors made from time series before and after a given point (the "split" case) to that calculated from two five vectors made respectively from the even and odd points (the "interlaced" case) revealed the culprit; the interlaced case, by imposing the same sequence of data gaps on both five vectors, eliminated this asymptotic error (see **Figure #5**, below) seen in all split case tests:

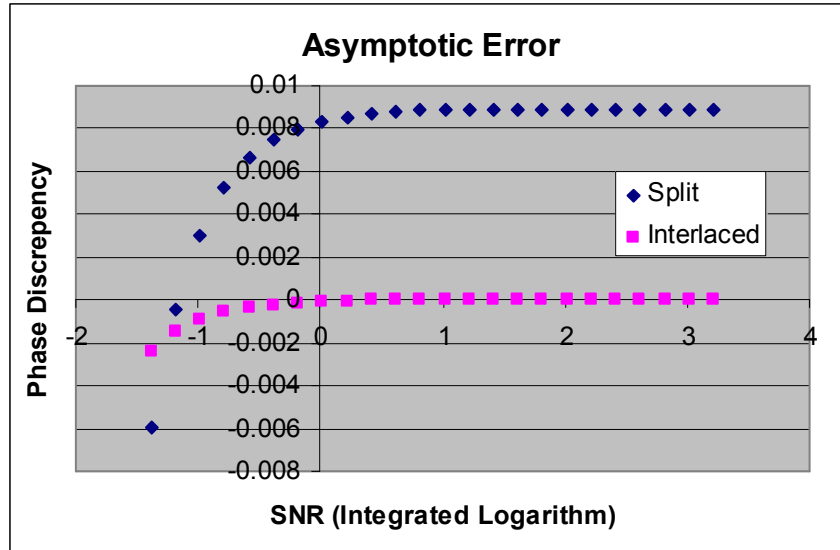


Figure #5: A comparison of the phase discrepancies recorded as a function of SNR for the split/interlaced test on simulated VIRGO data, with the presence of data holes and real scaled apparatus noise

Previous research by the VIRGO team at La Sapienza indicated similar effects appearing in CW target source parameter calculation due to the same effect; these results, by establishing a concrete precision limit even at high SNRs on real VIRGO data (which will even in advanced Virgo contain veto holes), make all the more imperative efforts to ameliorate hole effects. One proposal to this effect employs *data folding*, a technique in which the data from each day in the run are superimposed, removing all gaps not dependant on time of day. The effectiveness and robustness of this methodology remain open avenues for future research.

6.2 Performance Testing: multishift_tests.m

Performance testing on the multishift program was limited to tests using simulate VIRGO data scaled with real VIRGO background noise. Testing on the calculated phase shifts showed similarly impressive precision over the expected range of program use. The following graph (**Figure #6**) shows the results for these tests on a sequence of four one radian simulated phase shifts:

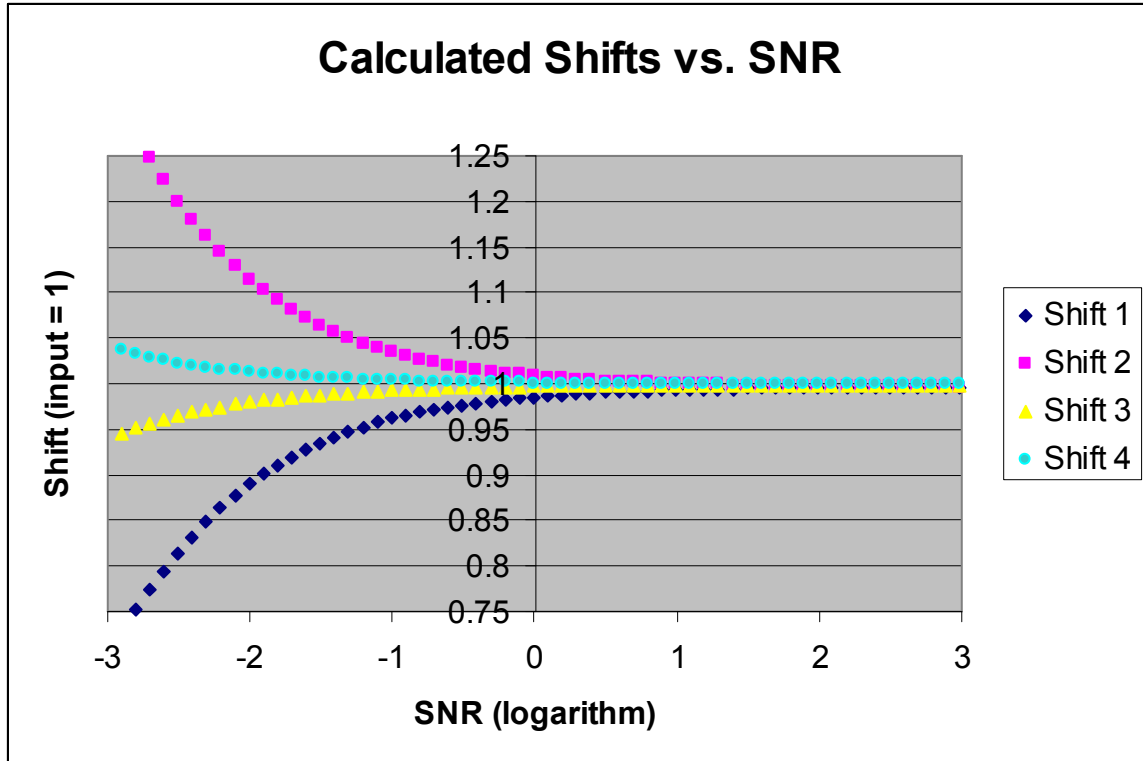


Figure #6: Calculated shifts for four one radian input shifts as a function of SNR. The curves appear as lines because the same noise was used at all point, with only the scale adjusted.

Issues, however, emerged during a second testing regimen, which probed the effect of the phase correction on the three other target source parameters, as well as the overall coherence. These test revealed that the time space correction, as originally envisioned, resulting in enormous and unpredictable changes in the estimates for η , ψ , and the magnitude, with size of the changes scaling with the size of the time shift. Though tests on this matter remain inconclusive, these effects seem to have stemmed from the loss of information relating to template calculation as a result of the shift in time used in the correction; removing this method of storage and switching to a frequency-space correction and output corrected this bug, rendering further testing on the time-space culprit essentially moot. In the current form, the phase correction has no effects (as expected) on the values of the other parameters.

6.3 Future Testing and Improvements

Due to the appearance of the parameter-effects bug discussed previously in section 6.2, the summer finished before progress could be made towards probing the effects of other parameter changes that might result from a pulsar glitch on the accuracy of `multishift_tests.m`. Similar to the SNR effects probe shown in **Figure #6**, an exploration of the effects of slight deviations in the values of η , ψ , and the magnitude across the glitch would yield a range of acceptable predicted changes for which the unadulterated program yields meaningful results. In this same vein, an η or ψ shift estimator could be grafted into the `multishift_test.m` framework, with individual coherence maximizations used for both parameters to estimate the change resulting from the pulsar glitch; such a change, however, would necessitate testing to ensure that

such wanton parameter correction does not compromise the coherence advantage of the 5N paradigm by greatly increasing the likelihood of a false positive.

The expiration of allotted time also prevented the full integration of the program `multishift_tests.m` into the existing Snag architecture. This along with the development of a protocol for use remains an essential, if somewhat minimal, step required prior to the formal research-scale examination of the gravitational radiation emitted by a glitch prone pulsar.

7. Conclusion

The programs produced during the course of this research demonstrated the ability to identify and correct for phase changes as might arise in VIRGO data due to the effects of a pulsar glitch. These programs perform their function in a manner consistent with the existing analysis structure, allowing for easy integration into the analysis stream. Future research into the area could employ these programs, or modifications thereof, as knowledge of the phenomenology surrounding pulsar glitches and their effect on gravitational radiation increases.

8. Acknowledgement

The author wishes to acknowledge the NSF (through the University of Florida) for funding, the University of Florida for facilitating the IREU, University La Sapienza in Rome for hosting with impeccable hospitality, and all the numerous researchers and administrators who made this summer possible, in particular his advisor, Dr. Christiano Palomba.

References:

- ¹ Flanagan, E. E. and S. A. Hughes. "The Basics of Gravitational Wave Theory." *New J. Phys.* **7** (2005) 204
- ² Taylor, J. H. and Weisberg, J. M. "Further Experimental Tests of Relativistic Gravity Using the Binary Pulsar PSR 1913+16" *Astrophys. Jour.* **345** (1989) 434-450.
- ³ Losurdo G. "Ground-based Gravitational Wave Interferometric Detectors of the First and Second Generation: An Overview" *Class. Quantum Grav.* **29** (2012) 124005
- ⁴ Acernese, F, et. al. "Status of VIRGO" *Class. Quantum Grav.* **21** (2004) S385–S394
- ⁵ Smith, J. R. "The Path to the Enhanced and Advanced LIGO Gravitational-Wave Detectors" *Class. Quantum Grav.* **26** (2009) 114013.
- ⁶ Willke, B. "GEO600: Status and Plans." *Class. Quantum Grav.* **24** (2007) S389–S397.
- ⁷ Davis, W. F. "Gravitational Radiation in the Brans-Dicke and Rosen Bi-metric Theories of Gravity with a Comparison to General Relativity." (Unpublished Doctoral Dissertation) MIT, Cambridge, MA, 1979.
- ⁸ New, K.C.B., et al. "Millisecond Pulsars: Detectable Sources of Continuous Gravitational Waves?" *Astrophys. J.* **450** (1995) 757-762.
- ⁹ Astone, P, et. al. "A Method for Detecting Known Sources of Continuous Gravitational Wave Signals in Non-stationary Data." *Class. Quantum Grav.* **27** (2010) 194016.
- ¹⁰ Astone, P, 2010.
- ¹¹ Astone, P, 2010.
- ¹² Astone, P, et al. "Coherent Search of Continuous Gravitational Wave Signals: Extension of the 5-vectors Method to a Network of Detectors." (Unpublished Paper) 2011.
- ¹³ Astone, 2010.
- ¹⁴ Espinoza, C. M., et al. "A study of 315 glitches in the rotation of 102 pulsars." *Mon. Not. R. Astron. Soc.* **414**, 1679–1704 (2011)
- ¹⁵ Middleditch, J. "Predicting the Starquakes in PSR J0537-6910" *Astrophys. J.* **652**: (2006) 1531-1546.
- ¹⁶ Astone, 2011